

Review

Mesoporous Transition Metal Oxides for Supercapacitors

Yan Wang ¹, Jin Guo ², Tingfeng Wang ², Junfeng Shao ², Dong Wang ² and Ying-Wei Yang ^{1,*}

¹ College of Chemistry, International Joint Research Laboratory of Nano-Micro Architecture Chemistry (NMAC), State Key Laboratory of Inorganic Synthesis and Preparative Chemistry, Jilin University, 2699 Qianjin Street, Changchun 130012, China;

E-Mail: wangy2011@jlu.edu.cn

² State Key Laboratory of Laser Interaction with Matter, Changchun Institute of Optics, Fine Mechanics and Physics, Chinese Academy of Science, Changchun 130033, China;

E-Mails: guoj@ciomp.ac.cn (J.G.); wtfeng@sina.com (T.W.); shaojunfeng1984@163.com (J.S.); wangd@ciomp.com.cn (D.W.)

* Author to whom correspondence should be addressed; E-Mail: ywyang@jlu.edu.cn; Tel.: +86-431-8516-8468.

Academic Editors: Jordi Sort and Eva Pellicer

Received: 18 August 2015 / Accepted: 8 October 2015 / Published: 14 October 2015

Abstract: Recently, transition metal oxides, such as ruthenium oxide (RuO₂), manganese dioxide (MnO₂), nickel oxides (NiO) and cobalt oxide (Co₃O₄), have been widely investigated as electrode materials for pseudo-capacitors. In particular, these metal oxides with mesoporous structures have become very hot nanomaterials in the field of supercapacitors owing to their large specific surface areas and suitable pore size distributions. The high specific capacities of these mesoporous metal oxides are resulted from the effective contacts between electrode materials and electrolytes as well as fast transportation of ions and electrons in the bulk of electrode and at the interface of electrode and electrolyte. During the past decade, many achievements on mesoporous transition metal oxides have been made. In this mini-review, we select several typical nanomaterials, such as RuO₂, MnO₂, NiO, Co₃O₄ and nickel cobaltite (NiCo₂O₄), and briefly summarize the recent research progress of these mesoporous transition metal oxides-based electrodes in the field of supercapacitors.

Keywords: supercapacitor; pseudo-capacitor; transition metal oxides; specific capacity; mesoporous materials

1. Introduction

Energy crisis and environmental pollution have triggered the development of clean and renewable energy storage systems. Supercapacitors, also called electrochemical capacitors, are a novel type of charge energy storage devices in between traditional capacitors and batteries [1,2]. Compared with traditional capacitors, supercapacitors possess higher specific capacity and specific energy. Meanwhile, they exhibit higher specific power, shorter charging time, more efficient discharging than batteries, and they cause no pollution in the environment [3]. Although their energy density is 10 to 50 times lower than lithium ion batteries now, supercapacitors with a near unlimited cycle life are useful in the fields of power system, memory storage, and vehicle assistant equipment (Figure 1). For example, combining a supercapacitor and a battery in a single unit can create an electric vehicle with longer life, lower costs and more power. Based on the principle of energy storage, supercapacitors can be classified into electric double layer capacitors (EDLCs) and pseudo-capacitors [4]. EDLCs store charges using the very thin double layer structure formed at the interface between electrode and electrolyte, while pseudo-capacitors use fast and reversible redox reactions on the surface and bulk near the surface of electrodes for energy storage. Compared with EDLCs, pseudo-capacitors exhibit higher capacitance and higher energy density [4–6].



Figure 1. Some possible applications of supercapacitors in today's society.

Nanoporous carbons are considered as one kind of ideal electrode materials for the EDLCs due to their large surface area, controlled pore structure, and high conductivity [7–9]. While for pseudo-capacitors, transition metal oxides as well as conducting polymers are common electrode materials [3]. Among them, transition metal oxides, such as ruthenium oxide (RuO_2), manganese dioxide (MnO_2), nickel oxides (NiO) and cobalt oxide (Co_3O_4), are investigated widely as electrodes materials [10–12]; both

faradaic and non-faradaic mechanisms are involved in charge storage [13–16]. RuO₂ involves faradaic charge-transfer reactions, and its cyclic voltammogram (CV) shape is quite broad, exhibiting a quasi-rectangular shape [17]. The good conductivity, rapid proton transport and larger surface area all contribute to rapid and reversible faradaic reactions with high capacitance [18]. Unfortunately, the high cost of RuO₂ limits its large-scale applications. Therefore, significant efforts are being focused on finding a promising alternative to RuO₂. MnO₂, NiO, and Co₃O₄ are investigated as electrode materials to replace RuO₂. MnO₂ possesses low cost and rectangular voltammogram due to fast and reversible faradaic reactions [19,20], which is taken as one of the promising alternatives to RuO₂. NiO, and Co₃O₄ are battery materials in the bulk state. When storage sites are limited on the surface of materials through nanostructure, significant pseudo-capacitance emerges [17]. Moreover, nickel cobaltite (NiCo₂O₄) also exhibits high capacitance values at short charge-discharge times recently, and redox behaviors of both nickel and cobalt are involved in energy storage [21,22]. Herein, RuO₂, MnO₂, NiO, Co₃O₄ and NiCo₂O₄ are specially selected, and their roles in supercapacitors will be reviewed.

A supercapacitor consists of electrode, electrolyte and separator, where electrode plays a key role for the performance of supercapacitor. It is a crucial task to explore electrode materials with excellent performance. According to the work principle of pseudo-capacitors, electrode materials and electrolyte should contact effectively, meanwhile, ions/charges should transport fast in the bulk of electrode and at the interface between electrode and electrolyte in order to achieve excellent properties. Therefore, transition metal oxides with mesopores (between 2 and 50 nm) are favorable for building supercapacitors with high performance due to their large specific surface area and suitable pore size distribution [23]. During the past decade, mesoporous RuO₂, MnO₂, NiO, Co₃O₄, and NiCo₂O₄ have been widely studied for supercapacitors. The simple and effective synthetic routes were developed, the nanomaterials with different morphologies were prepared, and the specific capacity and stability of devices were significantly improved. In this review, we briefly summarize the recent progress on these mesoporous transition metal oxide-based electrodes in the field of supercapacitors.

2. Transition Metal Oxides for Pseudo-Capacitors

2.1. Ruthenium Oxide (RuO₂) for Pseudo-Capacitors

RuO₂ is known as the best electrode material due to its large specific capacitance (700 F·g⁻¹), low resistivity, high chemical and thermal stability [18,24,25]. When RuO₂ is used as an electrode material, a series of redox processes occur, resulting in the variation of oxidation state among Ru⁴⁺, Ru³⁺ and Ru²⁺, where pseudo-capacitance mainly contributes to capacitance. Another feature is that these redox processes of RuO₂ are reversible. These unique electrochemical features result in quasi-rectangular shape CV curve (Figure 2). Due to these remarkable advantages, RuO₂, especially mesoporous RuO₂, has attracted much attention from scientific community and industry. Until now, several different routes have been developed for the synthesis of mesoporous RuO₂. For example, Galizzioli and Rochefort synthesized RuO₂ by thermal decomposition of RuCl₃ on metallic supports in solutions of electrolytes [26,27]. Zheng *et al.* prepared hydrous RuO₂ by a sol-gel process and obtained specific capacitance as high as 720 F·g⁻¹ for a powder formed at 150 °C [18]. This is the highest specific capacitance for RuO₂. In addition, Liu *et al.* prepared RuO₂ films by thermal and

electrochemical methods [28]. Dubala and coworkers reported a surfactant-less and binder-free chemical bath deposition method to synthesize RuO₂ thin films [29]. Although RuO₂ has large specific capacitance, it is difficult to use RuO₂ in real application, considering its very high cost and environmental toxicity. These limitations can be partly overcome by hybridization of RuO₂ with other common conductive materials. For instance, NiO/RuO₂ composite materials were prepared and a maximum specific capacitance of 210 F·g⁻¹ was obtained for composite electrode with 10 wt % RuO₂ in the voltage range of -0.4 to 0.5 V in 1 M KOH solution [30]. SnO₂/RuO₂ composite films were prepared by chemical bath deposition method. The specific capacitance of 150 F·g⁻¹ was obtained by optimizing synthetic conditions [31]. RuO₂/polyaniline electrodes were prepared by electrodeposition, revealing a specific capacitance of 474 F·g⁻¹ and a small charge transfer resistance of 2.24 Ω [32]. RuO₂/TiO₂ nanotubes composites were synthesized by loading various amounts of RuO₂ on TiO₂ nanotubes and a maximum specific capacitance of 1263 F·g⁻¹ was obtained [33]. By using carbon fibre paper as a support for RuO₂, a specific capacitance of 977 F·g⁻¹ was also obtained in a supercapacitor with 1M H₂SO₄ as electrolyte [34]. The special capacitances of these hybrid materials are summarized in Table 1.

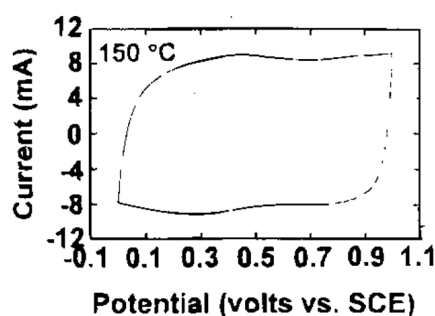


Figure 2. Cyclic voltammogram (CV) of RuO₂·xH₂O electrodes annealed at 150 °C. The voltage scan rate was 2 mV·s⁻¹, and the electrolyte was 0.5 M of H₂SO₄ [18].

Table 1. The special capacitances of hybrid RuO₂ materials.

Materials	Special Capacitance (F·g ⁻¹)
RuO ₂	720 [18]
NiO ₂ /RuO ₂	210 [30]
SnO ₂ /RuO ₂	150 [31]
RuO ₂ /Polyaniline	474 [32]
RuO ₂ /TiO ₂	1263 [33]
RuO ₂ /Carbon fibre paper	977 [34]

2.2. Manganese Dioxide (MnO₂) for Pseudo-Capacitors

MnO₂ has been taken as a promising alternative to RuO₂ because of its low cost and superior electrochemical performance [19,20,35,36]. Generally, capacitance properties of MnO₂ are investigated in Na₂SO₄ electrolyte. In Na₂SO₄ electrolyte, reversible transitions of MnO₂ ↔ MnOONa occur, which is responsible for pseudo-capacitance properties [19,20]. The rectangular voltammogram implies fast and reversible capacitive behaviors, which, together with excellent cycle stability of MnO₂, were demonstrated from the linearship of galvanostatic charge/discharge (GCD) profiles (Figure 3). According

to theoretical calculation, specific capacitance of MnO_2 is up to $1100 \text{ F}\cdot\text{g}^{-1}$ over a potential window of 1.0 V. However, the specific capacitances from experiments were five or ten times lower than theoretical values [37–41]. Both crystallographic forms (such as α , β , γ , δ , λ , *etc.*) and morphological nature are contributed to the low specific capacitance [37]. In order to obtain MnO_2 with high specific capacitance, much effort has been devoted to the synthesis of mesoporous MnO_2 . Template method, microemulsion method, hydrothermal method, sonochemical method and ultrasound irradiation have been utilized to synthesize mesoporous MnO_2 [38–41]. For example, semicrystalline gyroidal mesoporous MnO_2 was prepared by using mesoporous silica KIT-6 as hard template, and stable reversible electrochemical behavior with capacitance of $220 \text{ F}\cdot\text{g}^{-1}$ in a potential range of -0.1 – 0.55 V was observed [38]. Mesoporous MnO_2 nanoparticles with 4–5 nm of pore size were synthesized by a soft template method, and specific capacitance of $297 \text{ F}\cdot\text{g}^{-1}$ was obtained at a high loading level of $1.55 \text{ mg}\cdot\text{cm}^{-2}$ [39]. Mesoporous MnO_2 with 2–20 nm of average pore sizes were obtained in sonochemical method from KMnO_4 by using a tri-block copolymer (P123) as a soft template, and a maximum specific capacitance of $265 \text{ F}\cdot\text{g}^{-1}$ was obtained (Figure 4a,b) [40]. Mesoporous MnO_2 with specific surface area of $192 \text{ m}^2\cdot\text{g}^{-1}$ and 10 nm of pore distribution was synthesized through the reaction of potassium permanganate and ethanol under ultrasound irradiation (Figure 4c,d). The specific capacitance of $229 \text{ F}\cdot\text{g}^{-1}$ and the specific capacitance retention of 97.3% after 2000 cycles were obtained [19]. Birnessite-type mesoporous MnO_2 nanospheres were synthesized by the microwave-hydrothermal method, and the electrochemical test showed that the specific capacitance was $210 \text{ F}\cdot\text{g}^{-1}$ at $200 \text{ mA}\cdot\text{g}^{-1}$ in 1.0 M Na_2SO_4 electrolyte with the specific capacitance retention and columbic efficiency of over 96% and 98%, respectively, after 300 cycles at $1.6 \text{ A}\cdot\text{g}^{-1}$ [41].

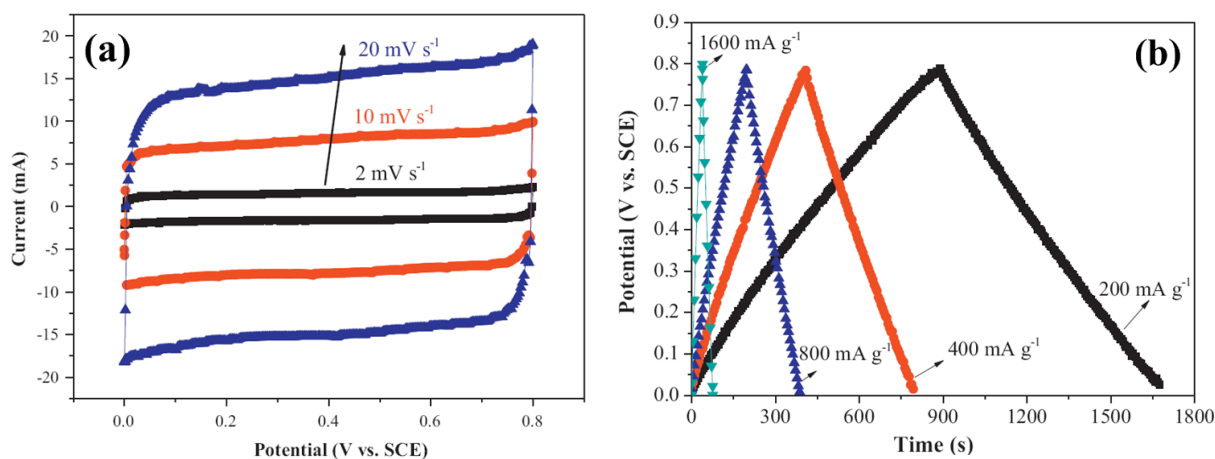


Figure 3. (a) CVs of MnO_2 at scan rates of 2, 10, and $20 \text{ mV}\cdot\text{s}^{-1}$; and (b) Galvanostatic charge/discharge (GCDs) of MnO_2 at current densities of 200, 400, 800, and $1600 \text{ mA}\cdot\text{g}^{-1}$ [41].

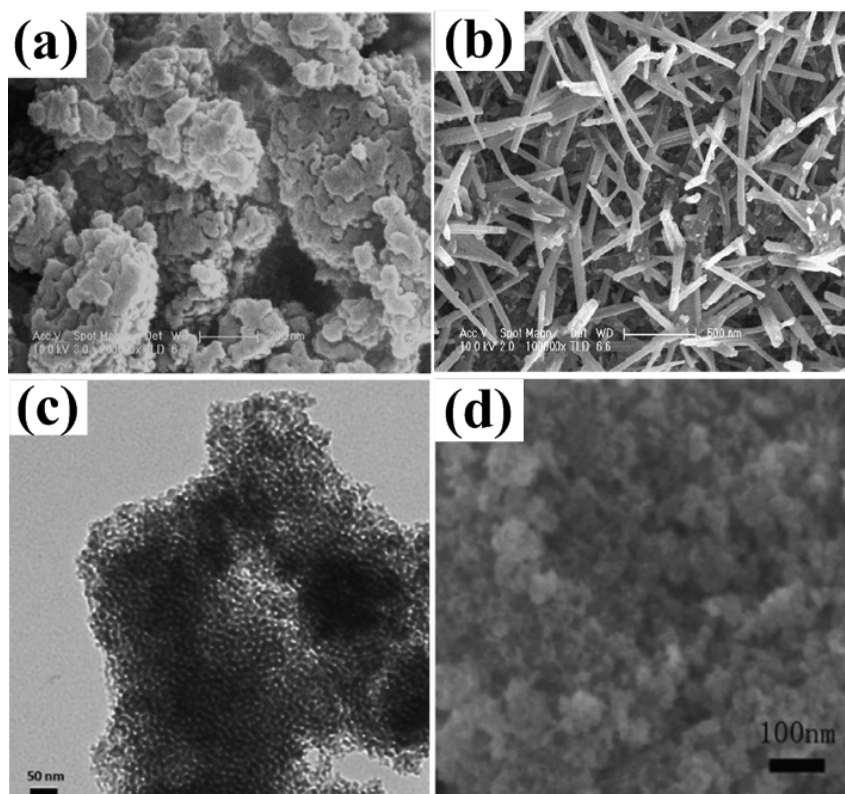


Figure 4. Scanning electron microscopy (SEM) images of MnO₂ samples synthesized by sonochemical method with two different amplitudes: (a) 30 μm; (b) 60 μm [34]. Transmission electron microscope (TEM) (c) and SEM (d) images of mesoporous MnO₂ synthesized through the reaction of potassium permanganate and ethanol under ultrasound irradiation [19].

2.3. Nickel Oxide (NiO) for Pseudo-Capacitors

NiO is regarded as a promising pseudo-capacitor material due to its high theoretical capacitance value of 2573 F·g⁻¹, low cost and distinct redox [42]. For NiO, the variation of oxidation state of Ni is still not very clear. The reaction, NiO + OH ↔ NiOOH + e⁻, is usually believed to occur first. Then, the oxyhydroxide participates in the following reversible redox processes [17]. There are still some issues to be solved for the practical applications of NiO in supercapacitors. Among them, the significantly lower specific capacitance than theoretical value is one of the main issues. Due to the tight correlation between electrochemical performance of NiO and its porosity and surface area, most of the recent works are focused on the synthetic method and morphology study of materials. It has been known that mesoporous structured transition metal oxides are favorable for specific capacitance. On one hand, large specific surface is beneficial for electrolytes to access the electrochemically active sites. On the other hand, the mesoporous pore size is profitable for fast redox process. For the preparation of NiO with mesoporous structures, several methods have been employed. For example:

(1) Ni(OH)₂ → NiO: Wu *et al.* prepared highly porous NiO via a combination of sol-gel process with supercritical drying method [5]. They prepared aerogel-like Ni(OH)₂ samples and then heated them to achieve aerogel-like NiO. The as-synthesized NiO samples exhibited 80%–90% of porosity and 180.5–325.6 m²·g⁻¹ of surface area. The average specific capacitance was observed to be *ca.* 75–125 F·g⁻¹

between a potential window of 0–0.35 V vs. SCE [5]. Yuan and coworkers synthesized β -Ni(OH)₂ microspheres by using coalescence and Ostwald-ripening mechanisms, and then these β -Ni(OH)₂ microspheres were calcinated to produce hierarchical porous NiO microsphere (Figure 5a–d) [41]. Electrochemical data demonstrated that the hierarchical porous NiO nano/micro superstructures were capable of delivering a specific capacitance of 710 F·g⁻¹ at 1 A·g⁻¹ and offered a specific capacitance retention of *ca.* 98% after 2000 continuous charge-discharge cycles [43]. Lee *et al.* applied hexamethylenetetramine hydrolysis to synthesize Ni(OH)₂ microstructures, followed by calcination to produce NiO microstructures at high temperature. The specific capacitance of fabricated NiO at 2, 5, 10, and 20 mV·s⁻¹ scan rate was 718, 470, 420, and 403 F·g⁻¹, respectively. The NiO microstructures had good retention for more than 1000 cycles in a cycling test [44].

(2) Hydrothermal Method: Li *et al.* used hydrothermal route to synthesize Ni(OH)₂, and then prepared various mesoporous NiO hierarchical microspheres via thermal decomposition of Ni(OH)₂ in air [45]. Electrochemical data demonstrated that the mesoporous NiO network-like hierarchical microspheres could deliver a specific capacitance of 555 F·g⁻¹ at 2 A·g⁻¹, and 390 F·g⁻¹ even at a current density of 10 A·g⁻¹ [45]. Yang *et al.* prepared mesoporous slit-structured NiO materials through a hydrothermal route with sodium dodecyl benzene sulfonate (SDBS) as an additive (Figure 5e–f). The as-prepared NiO samples presented specific capacitance of over 1700 F·g⁻¹ in the potential range from 0.10 to 0.56 V at a constant current of 2 A·g⁻¹, and capacitance retention of 90% after 1000 continuous charge-discharge cycles [46].

(3) Template Method: Mesoporous NiO was synthesized by a hydrothermal homogeneous precipitation method using mixed anionic/non-ionic surfactants as template. The electrochemical results showed that the as-prepared mesoporous NiO sample had a specific capacitance of 268 F·g⁻¹ [47]. A nanospherical porous NiO electrode material was prepared by using porous carbon nanospheres as a hard template (Figure 5g–j). The GCD measurements demonstrated that the optimal electrode possessed a specific capacitance of 1201 F·g⁻¹ at a discharge current density of 0.5 A·g⁻¹ and cycling stability of 70% capacity retention after 500 continuous charge/discharge cycles [48].

(4) Microwave Assisted Heating Method: Meher *et al.* prepared porous NiO by microwave assisted heating method under homogeneous precipitation conditions [49]. Compared with that from the traditional reflux method, the sample prepared from microwave method showed higher rate specific capacitance (370 F·g⁻¹) in the charge-discharge measurements made at a discharge current of 2 A·g⁻¹ [49].

(5) Sol-Gel Method: NiO nanostructures with three distinct morphologies were fabricated by a sol-gel method, and nanoflower-shaped NiO with a distinctive three-dimensional (3D) network showed good supercapacitor properties [50].

Another obstacle to specific capacitance of NiO is its poor conductivity, which results in low electron transport. To enhance electrochemical activity of the electrode, the dopants, such as transition and non-transition metal ions, have been introduced into the lattices of metal oxides. For instance, La³⁺ doped NiO microspheres with porous structures were fabricated using colloidal carbon spheres as hard template via a hydrothermal method followed by a calcination process. As a result, 1.5 mol% La³⁺ doped NiO showed a remarkable specific capacitance of 253 F·g⁻¹ (two times higher than that of the pure NiO) and good cycling stability (34% capacity increase after 500 cycles) (Figure 6) [51].

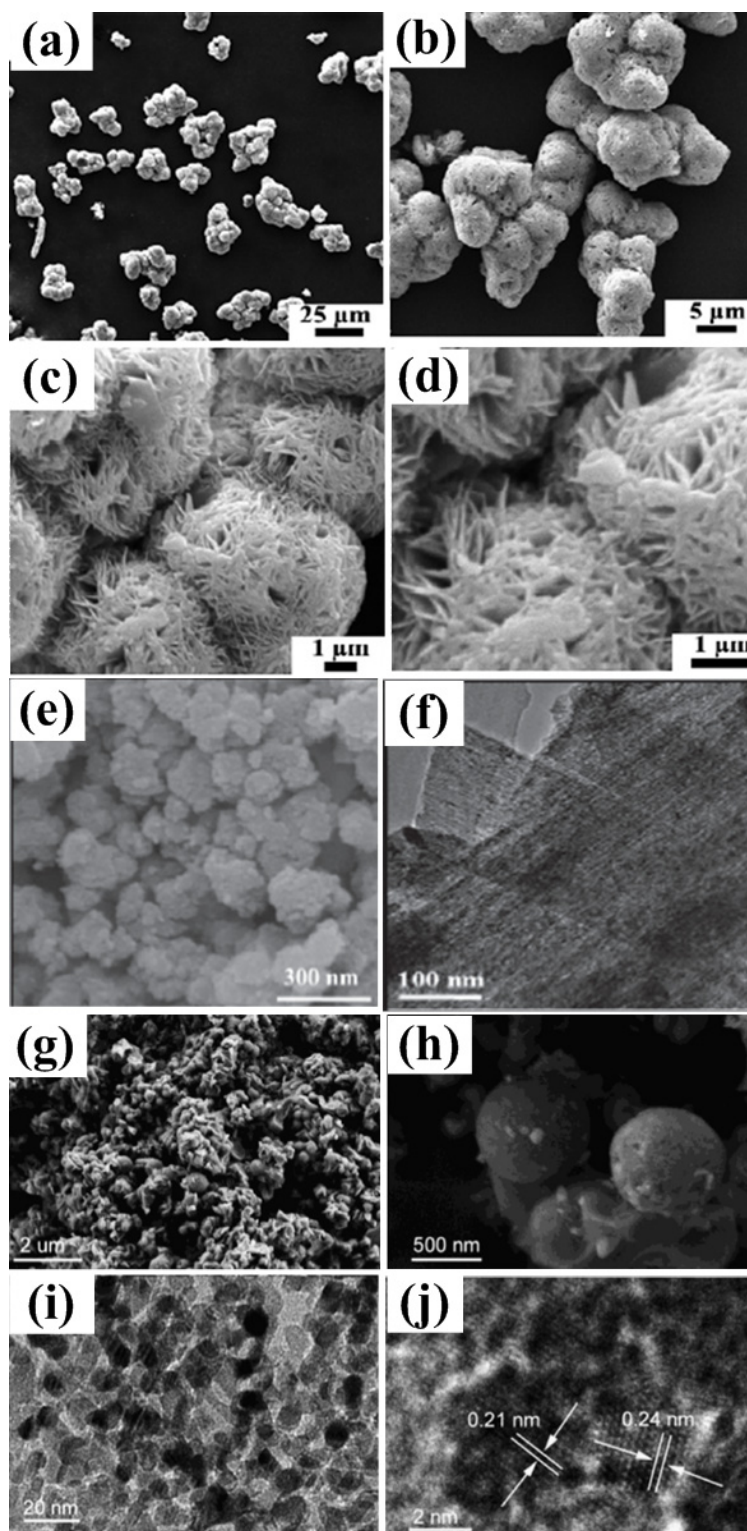


Figure 5. SEM images of the synthesized NiO microspheres (obtained by thermal decomposition of the $\text{Ni}(\text{OH})_2$ precursor after refluxing treatment for 60 min) at different magnifications (a–d) [43]. (e) SEM and (f) high resolution transmission electron microscopy (HRTEM) images of the NiO sample synthesized via a hydrothermal route with sodium dodecyl benzene sulfonate (SDBS) as an additive [46]. SEM images (g,h) at different magnifications, and TEM (i) and HRTEM (j) images of NiO sample prepared by using porous carbon nanospheres as a hard template [48].

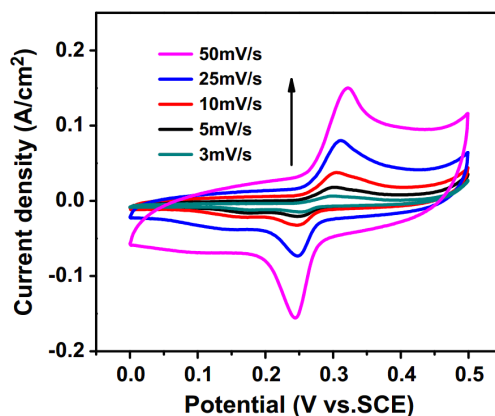


Figure 6. CVs of 1.50 mol% La³⁺-doped NiO electrode measured at scan rates from 3 to 50 mV·s⁻¹ [51].

There are also some reports on the synthesis of NiO/conductive materials. For example, monolithic NiO/Ni nanocomposite electrodes were fabricated recently, and the maximum capacitance was 910 F·g⁻¹ due to the highly activated NiO surface layer and the conductive network of metal cores [52]. Flower-shaped NiO/ α -Ni(OH)₂ hybrid structures were synthesized by a solvothermal process. The hybrid composite demonstrates a solid capacitance value of 707 F·g⁻¹ at 2 A·g⁻¹ and 474 F·g⁻¹ at a high discharge rate of 10 A·g⁻¹. In order to further improve the performance and the capacitance retention, conductive carbon nanomaterials were used as supports for the NiO/ α -Ni(OH)₂ hybrid and it was found that single-walled carbon nanotubes significantly enhanced the performance of composite to 810 F·g⁻¹ at a high current discharge of 10 A·g⁻¹ [42].

2.4. Cobalt Oxide (Co₃O₄) for Pseudo-Capacitors

Co₃O₄ has low environmental toxicity and high specific capacitance of 3560 F·g⁻¹ in theory, and is of low cost [53,54]. During electrochemical processes, both pseudocapacitive behavior (CoOOH + OH⁻ ↔ CoO₂ + H₂O + e⁻) and battery-type behavior (Co₃O₄ + OH⁻ + H₂O ↔ 3MOOH + e⁻) are contributed to capacitance, which results in high capacitance values (3560 F·g⁻¹ in theory) [17,53,54]. However, the specific capacitances from real devices are much lower than that from theory. Electron effective transportation and ion fast diffusion would result in high performance of supercapacitors. Therefore, much effort has been devoted to synthesizing Co₃O₄ with appropriate nanostructures, particularly, Co₃O₄ nanomaterials with mesoporous structures, to improve the electron and ion transportation in electrodes and at the interface between electrode and electrolyte in supercapacitor devices [55,56]. For example, mesoporous nanocrystalline Co₃O₄ with a particle diameter of *ca.* 3 nm was synthesized based on strong chemical coordination interactions between Co²⁺ in solution and amino groups in the polyacrylamide template, and capacitance of 401 F·g⁻¹ was obtained from these prerequisites [57]. Mesoporous Co₃O₄ microspheres with crater-like morphology were obtained by utilizing the mesoporous silica material named MCM-41 as a template. This material provided a specific capacitance of 102 F·g⁻¹ and capacity retention of 74% in 500 continuous cycles test at a sweep rate of 3 mV·s⁻¹ [58]. Hierarchically porous Co₃O₄ film was prepared by electrodeposition via liquid crystalline template, and specific capacitances of these Co₃O₄ films were 443 F·g⁻¹ at 2 A·g⁻¹ and 334 F·g⁻¹ at 40 A·g⁻¹, respectively [59]. Ultrafine nanosized Co₃O₄ materials with interconnected

macroporous and mesoporous structure were synthesized through sol-gel method, followed by freeze-drying. The specific capacitance of the Co_3O_4 material was $742.3 \text{ F}\cdot\text{g}^{-1}$ at a scan rate of $5 \text{ mV}\cdot\text{s}^{-1}$ and the capacity retention was 86.2% after 2000 cycles [60]. With the assistance of mesoporous carbon nanorods, Co_3O_4 nanocubes with uniform diameter and high crystallinity were obtained. After calcination, mesoporous Co_3O_4 nanocubes were formed. Electrochemical tests revealed that the specific capacitance of Co_3O_4 nanocube electrode is *ca.* $350 \text{ F}\cdot\text{g}^{-1}$ at the current densities of $0.2 \text{ A}\cdot\text{g}^{-1}$ (Figure 7) [61]. In addition, mesoporous Co_3O_4 with other morphologies were also prepared. For example, tubular Co_3O_4 was fabricated by biomorphic synthesis route [62], nanosheets Co_3O_4 and microspheres Co_3O_4 were prepared by an ethanolamine-assisted solvothermal method and sequential thermal decomposition at atmospheric pressure [63].

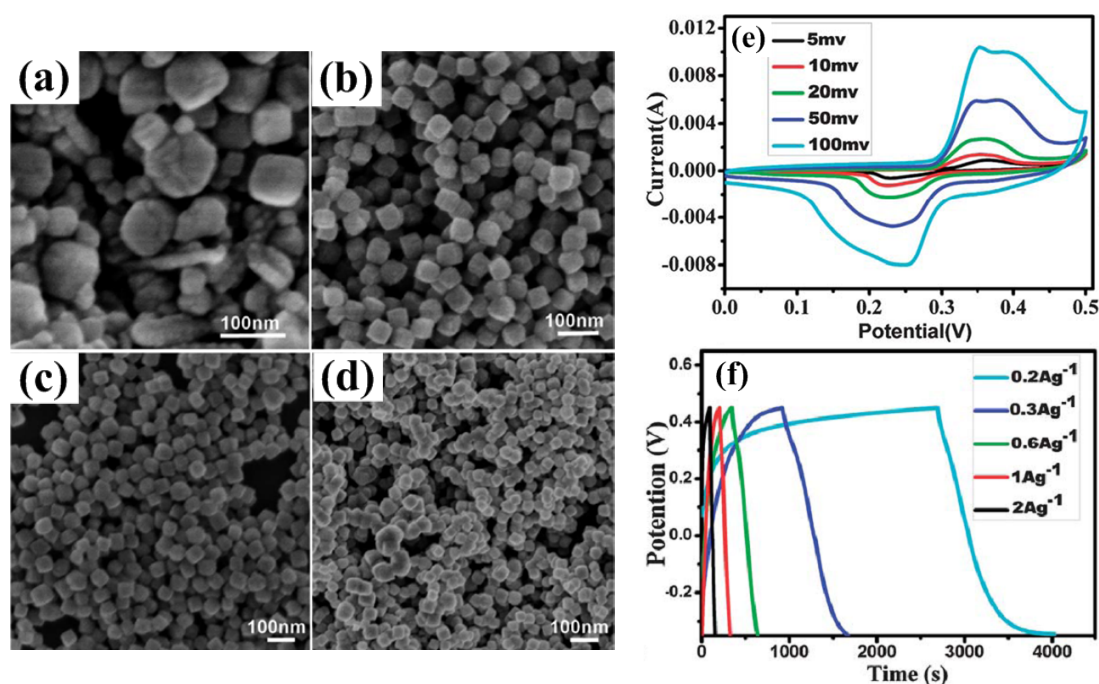


Figure 7. SEM images of Co_3O_4 samples obtained by adding different concentrations of mesoporous carbon nanorods: (a) $0 \text{ mg}\cdot\text{mL}^{-1}$; (b) $0.0175 \text{ mg}\cdot\text{mL}^{-1}$; (c) $0.025 \text{ mg}\cdot\text{mL}^{-1}$; (d) $0.05 \text{ mg}\cdot\text{mL}^{-1}$. (e) CV curves of the mesoporous Co_3O_4 nanocube electrode at scan rates of 5, 10, 20, 50 and $100 \text{ mV}\cdot\text{s}^{-1}$ and (f) galvanostatic charge/discharge (GCD) curves of the as-prepared electrode at different current densities [61].

In order to simplify the synthetic route and improve the electrochemical performance, mesoporous Co_3O_4 was grown on some support materials to form hybrid structures. For example, ultrathin mesoporous Co_3O_4 nanosheet arrays were grown on Ni foam with robust adhesion, which endows fast ion and electron transport, large electroactive surface area, and good structural stability. As a result, superior pseudo-capacitive performance was achieved with ultrahigh specific capacitance in the range of $2735\text{--}1471 \text{ F}\cdot\text{g}^{-1}$ and excellent cycling stability up to 3000 cycles (Figure 8) [64]. Co_3O_4 was embedded into SBA-15 nanoparticles to form composites by wetness impregnation method (Figure 9). The composite structure improves charged ion transmission inside the channels and the electrochemical utilization of Co_3O_4 during the charge/discharge processes. A supercapacitor electrode material based on $\text{Co}_3\text{O}_4(66\%)\text{@SBA-15}$ exhibited a maximum specific capacitance of $1086 \text{ F}\cdot\text{g}^{-1}$ in 6 M KOH

solution. After 10 000 cycles, retention of 90% of the initial capacitance was observed (Figure 9) [65]. Co_3O_4 nanowire/nanoflower hybrid structure on carbon fibre cloth was prepared via a hydrothermal approach followed by thermal treatment in air (Figure 10). A supercapacitor made from this hierarchical hybrid architecture showed a maximum specific capacitance of $4.8 \text{ mF}\cdot\text{cm}^{-2}$ at a constant density of $3 \text{ mA}\cdot\text{cm}^{-2}$ in organic electrolyte. In terms of energy and power, the supercapacitor conveyed an energy density of $4.2 \text{ mW}\cdot\text{h}\cdot\text{cm}^{-3}$ with a power density of $1260\cdot\text{mW}\cdot\text{cm}^{-3}$ [66].

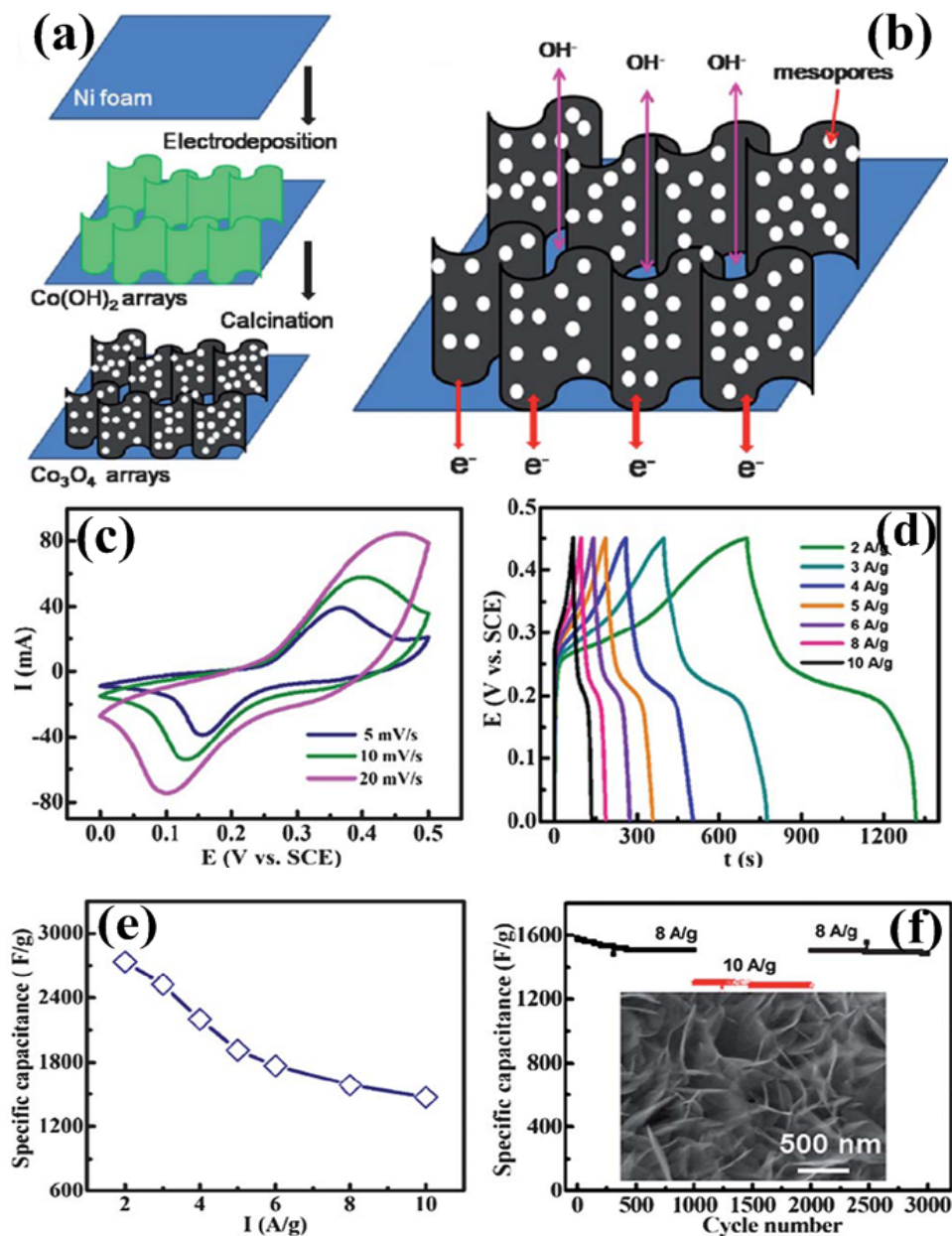


Figure 8. Schematic illustrations of (a) the general electrode design process; and (b) the application advantages of building 2D mesoporous Co_3O_4 ultrathin nanosheet arrays on Ni foam; (c) CV curves; (d) charge-discharge curves; (e) specific capacitance *versus* current densities; and (f) cycling performance of the Co_3O_4 nanosheet arrays/Ni foam electrode at varying current densities. The inset in (f) is field emission scanning electron microscope (FESEM) image of the Co_3O_4 nanosheet arrays/Ni foam electrode after cycling [64].

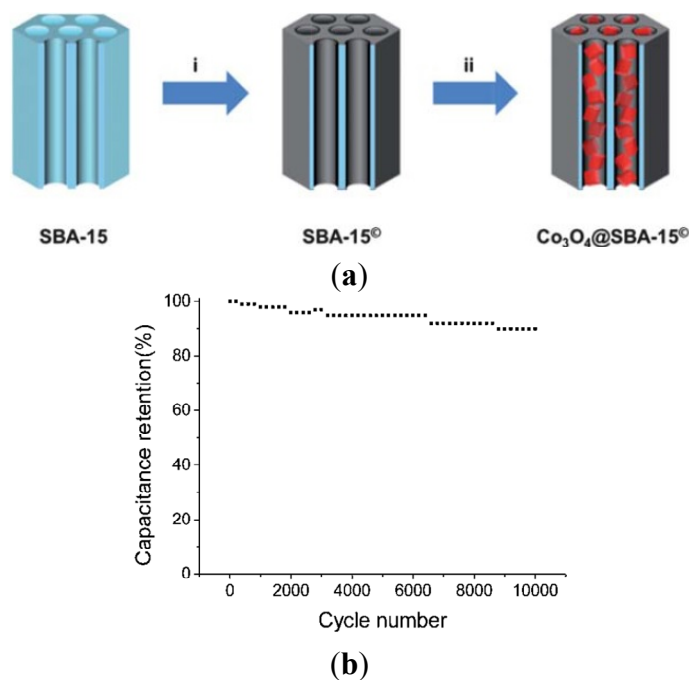


Figure 9. (a) Illustration of the preparation of $\text{Co}_3\text{O}_4@\text{SBA-15}$ supercapacitor electrode materials, showing (i) carbon nanomembrane (dark gray) formation on the walls (gray blue) of SBA-15 and (ii) incorporation of Co_3O_4 clusters into the cylinder type mesochannels and (b) cycle life of $\text{Co}_3\text{O}_4(66\%)@\text{SBA-15}$ electrode material at a scan rate of $0.1 \text{ V}\cdot\text{s}^{-1}$ [65].

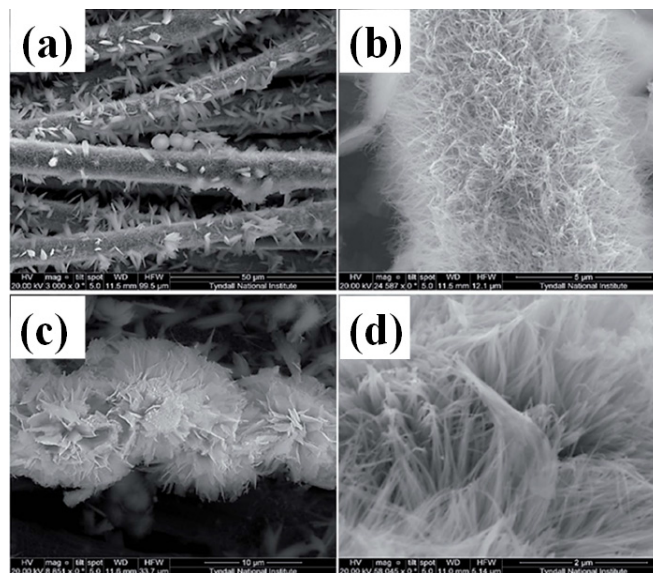


Figure 10. HRSEM images of Co_3O_4 nanowire/nanoflower on carbon fibre cloth at different magnifications [66]. (a) and (b) are the low magnification SEM images of bundles of carbon fibers; (c) and (d) are the high magnification SEM images.

2.5. Nickel Cobaltite (NiCo_2O_4) for Pseudo-Capacitors

From the above discussion, one can see that NiO and Co_3O_4 have attracted wide interest recently in supercapacitor applications due to their high theoretical capacity, abundant structure, good stability

and low cost. However, in real supercapacitor devices, the observed specific capacitances are still far lower than theoretical values, especially at high rates [67]. A novel compound, NiCo_2O_4 , attracts researchers' attention. In 2010, Wei *et al.* obtained its specific capacitance as high as $1400 \text{ F}\cdot\text{g}^{-1}$ at a sweep rate of $25 \text{ mV}\cdot\text{s}^{-1}$ in a 1 M NaOH solution within a potential window of 0.04–0.52 V [68]. After that, NiCo_2O_4 has been extensively investigated for pseudo-capacitors. NiCo_2O_4 possesses good electrochemical activity and electrical conductivity at least two orders of magnitude higher than pure Co_3O_4 and NiO [69]. Both nickel and cobalt ions are involved in redox reactions, which is richer than pure nickel oxides and cobalt oxides. The energy storage occurs with reversible transformation of NiCo_2O_4 into nickel and cobalt oxyhydroxides as well as the reversible redox reaction of $\text{CoOOH} + \text{OH}^- \leftrightarrow \text{CoO}_2 + \text{H}_2\text{O} + \text{e}^-$. The theoretical capacity for NiCo_2O_4 , including the pseudocapacitive and the battery-like faradaic contributions, is $1203 \text{ C}\cdot\text{g}^{-1}$ or $2005 \text{ F}\cdot\text{g}^{-1}$ assuming at 0.6 V potential window in an aqueous alkaline electrolyte [22]. Up to now, NiCo_2O_4 with different structures and morphology, different dimensions have been reported and their electrochemical performances were improved greatly. For example, one-dimensional (1D) ultralayered mesoporous NiCo_2O_4 nanowires were synthesized by a template-free strategy (Figure 11). The ultralayered mesoporous nanowire electrode exhibited specific capacitance of $401 \text{ F}\cdot\text{g}^{-1}$ at $1 \text{ A}\cdot\text{g}^{-1}$ and excellent cycling stability (only *ca.* 10% loss after 5000 cycles) [70]. Mesoporous NiCo_2O_4 nanostructure was synthesized via a D-glucose-assisted solvothermal process. Electrochemical measurements showed that the spinel NiCo_2O_4 nanostructure heated at $300 \text{ }^\circ\text{C}$ exhibited maximum specific capacitances of $524 \text{ F}\cdot\text{g}^{-1}$ at $0.5 \text{ A}\cdot\text{g}^{-1}$ and $419 \text{ F}\cdot\text{g}^{-1}$ at $10 \text{ A}\cdot\text{g}^{-1}$ with good cycle stability and only $\sim 9\%$ of capacitance loss after 2500 cycles [71]. Hierarchical mesoporous spinel NiCo_2O_4 was synthesized by a hydrothermal method assisted by polyvinylpyrrolidone (PVP) and a post annealing treatment. Compared to conventional flower-like NiCo_2O_4 , the hierarchical mesoporous structured NiCo_2O_4 exhibited better supercapacitance performance. The specific capacitance could reach $1619.1 \text{ F}\cdot\text{g}^{-1}$ at a current density of $2.0 \text{ A}\cdot\text{g}^{-1}$. When the current density was increased to $10.0 \text{ A}\cdot\text{g}^{-1}$, a specific capacitance of $571.4 \text{ F}\cdot\text{g}^{-1}$ could be obtained (Figure 12) [72]. Spinel NiCo_2O_4 was synthesized through a thermal decomposition method and specific capacitance was $764 \text{ F}\cdot\text{g}^{-1}$ at $2 \text{ mV}\cdot\text{s}^{-1}$ [73]. 3D network-like mesoporous NiCo_2O_4 nanostructures were fabricated through a solvothermal route coupled with a post annealing treatment. The as-obtained NiCo_2O_4 manifested specific capacitance of $931 \text{ F}\cdot\text{g}^{-1}$ at $3 \text{ A}\cdot\text{g}^{-1}$, capacity retention rate of 85.2 and 72.5% at 20 and $50 \text{ A}\cdot\text{g}^{-1}$, respectively [74].

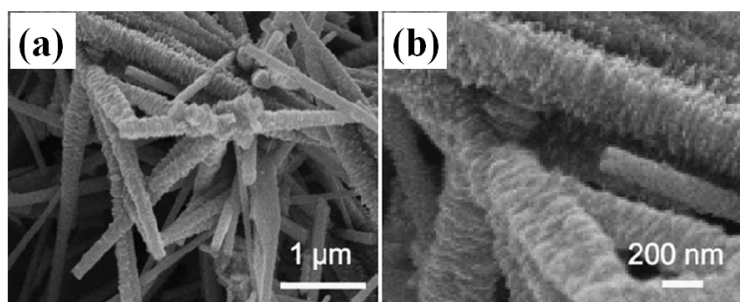


Figure 11. (a) and (b) FESEM images of the as-synthesized ultralayered mesoporous NiCo_2O_4 nanowires at different magnifications [70].

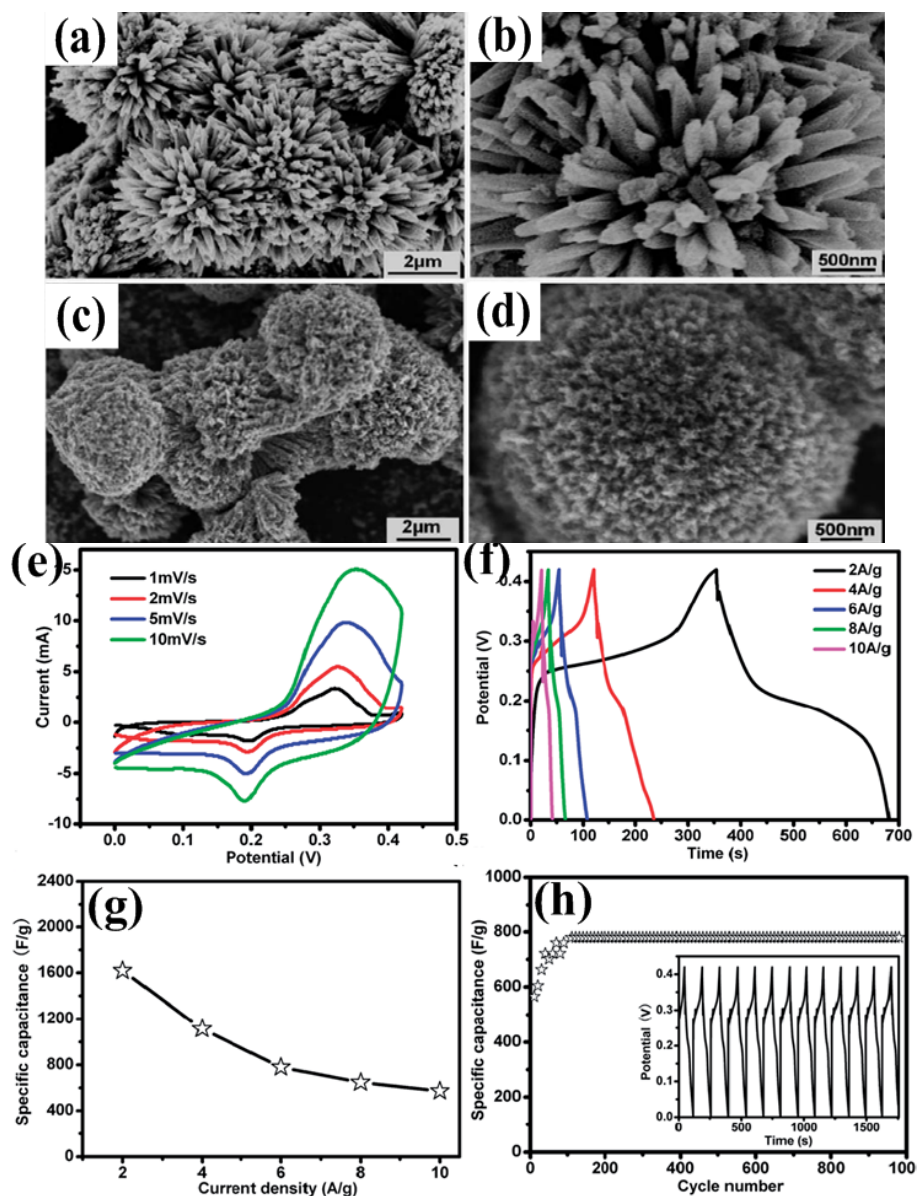


Figure 12. FESEM images of flower-like NiCo_2O_4 (a and b) and hierarchical mesoporous structured NiCo_2O_4 (c and d); electrochemical performance of hierarchical mesoporous NiCo_2O_4 electrodes. (e) CV curves at scan rates of 1.0, 2.0, 5.0 and 10.0 $\text{mV}\cdot\text{s}^{-1}$, respectively; (f) GCD curves at various current densities; (g) Effects of current density on its specific capacitance; (h) Cycling performance over 1000 cycles at a current density of 6.0 $\text{A}\cdot\text{g}^{-1}$. The inset shows the GCD curve at a current density of 6.0 $\text{A}\cdot\text{g}^{-1}$ [72].

In recent two years, the growth of NiCo_2O_4 on a conductive substrate attracts more and more attention. By this means, not only the conductivity of electrodes but also the specific surface areas is enhanced greatly. These unique composite electrodes may become ideal materials to improve the performance of pseudocapacitors. Several works have demonstrated the advantages of the composite electrodes. For example, mesoporous NiCo_2O_4 nanoneedles were grown on three-dimensional (3D) graphene-nickel foam and were then used to construct supercapacitor. The specific capacitance of NiCo_2O_4 nanoneedles was $1588 \text{ F}\cdot\text{g}^{-1}$ at $1 \text{ A}\cdot\text{g}^{-1}$ and the power density and energy density was $33.88 \text{ Wh}\cdot\text{kg}^{-1}$ at $5 \text{ kW}\cdot\text{kg}^{-1}$, respectively [75]. Hierarchical porous NiCo_2O_4 films composed of

nanowalls on nickel foam were synthesized via a facile hydrothermal method. A capacity of $130 \text{ mA}\cdot\text{h}\cdot\text{g}^{-1}$ was achieved at $2 \text{ A}\cdot\text{g}^{-1}$ with 97% capacity maintained after 2000 cycles [76]. NiCo_2O_4 multiple hierarchical structures composed of 1D nanowires and 2D nanosheets were grown on Ni foam. NiCo_2O_4 exhibited a specific capacitance of even up to $2623.3 \text{ F}\cdot\text{g}^{-1}$, scaled to the active mass of NiCo_2O_4 sample at a current density of $1 \text{ A}\cdot\text{g}^{-1}$. A nearly constant rate performance of 68% was achieved at a current density ranging from 1 to $40 \text{ A}\cdot\text{g}^{-1}$, and the sample retained approximately 94% of its maximum capacitance even after 3000 continuous charge-discharge cycles at a consistently high current density of $10 \text{ A}\cdot\text{g}^{-1}$ [77]. The ultrathin NiCo_2O_4 nanosheets supported on nickel foam were prepared via a two-step process, electrodeposition method followed with thermal treatment. The as-prepared samples were directly fabricated as electrodes for supercapacitors, and the outstanding electrochemical performance of $2517 \text{ F}\cdot\text{g}^{-1}$ was achieved at $1 \text{ A}\cdot\text{g}^{-1}$ and could still maintain $1200 \text{ F}\cdot\text{g}^{-1}$ at current density of $15 \text{ A}\cdot\text{g}^{-1}$. The cyclic stability was also tested under current density of $8 \text{ A}\cdot\text{g}^{-1}$, and 64% of initial capacitance was still maintained after 800 cycles [78].

Although transition metal oxides, such as RuO_2 , MnO_2 , NiO and Co_3O_4 , have been widely investigated for pseudo-capacitors, their practical applications are still limited due to their poor stability and low electrical conductivity [79]. While active carbon materials possess good conductivity and high stability. Thus, combining transition metal oxides with carbon materials may enhance the electric conductivity, and improve electrochemical performance of supercapacitors. Design and synthesis of transition metal oxides/active carbon materials were also reported [4,80–85]. For example, RuO_2 /ordered mesoporous carbon materials were prepared by impregnating an ordered mesoporous carbon CMK-3 with $\text{RuCl}_3\cdot x\text{H}_2\text{O}$ solution followed by annealing in nitrogen atmosphere. The annealing temperature and the RuO_2 content had great influence on the specific capacitance of composites. The highest specific capacitance reached $633 \text{ F}\cdot\text{g}^{-1}$ by adjusting synthetic conditions [4]. Metal oxide nanorods (MnO_2 , SnO_2 , NiO) inside mesoporous silica supported carbon nanomembranes (denoted as SS-CNM) were applied for electrodes to fabricate symmetrical supercapacitors. Owing to the high electrical conductivity of SS-CNM and the intimate contact between the carbon membrane and well-ordered metal oxide nanorods, specific capacitances of MnO_2 nanorods/SS-CNM, SnO_2 nanorods/SS-CNM, and NiO nanorods/SS-CNM were achieved to be 964, 745, and $620 \text{ F}\cdot\text{g}^{-1}$, respectively. In addition, less than 10% of capacitance decays over 10 000 circles and energy density was 33.5, 25.7, and $21.6 \text{ Wh}\cdot\text{kg}^{-1}$ for MnO_2 nanorods/SS-CNM, SnO_2 nanorods/SS-CNM, and NiO nanorods/SS-CNM, respectively (Figure 13) [79]. Mesoporous NiO /reduced graphene oxide composites were synthesized by a hydrothermal route. Because the 3D graphene conductive network and the mesoporous structure were favorable for charge transportation and electrolyte diffusion, NiO /RGO composites exhibited high specific capacitance ($1016.6 \text{ F}\cdot\text{g}^{-1}$) and good cycling stability (94.9% capacitance retention after 5000 cycles) [85].

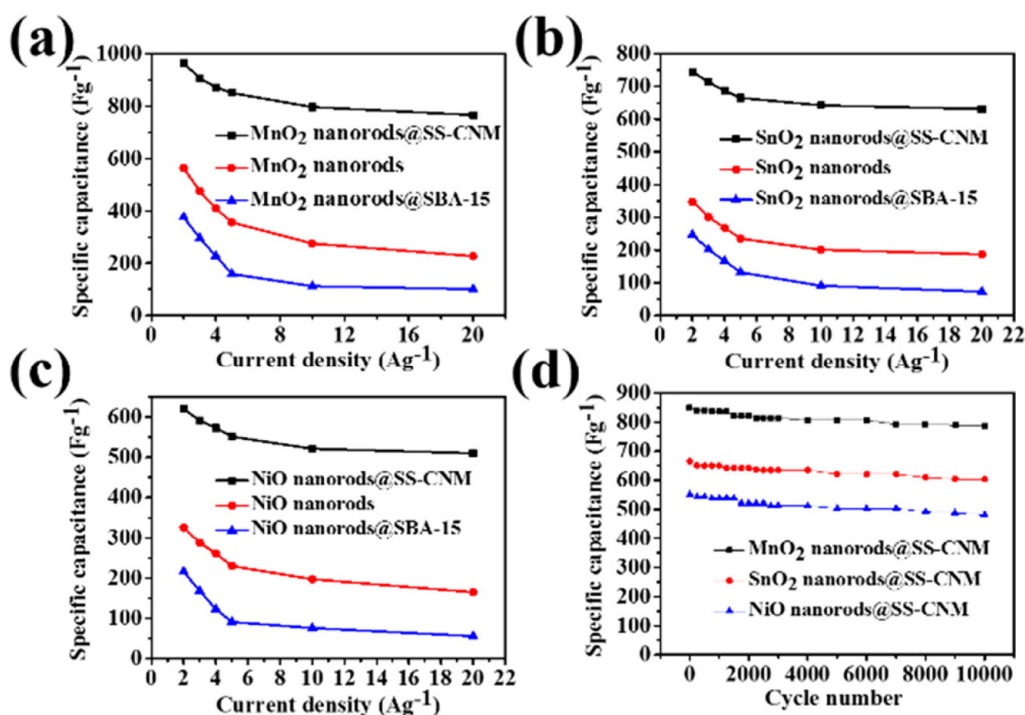


Figure 13. Curves of specific capacitance *versus* varied current density of MnO₂ nanorods@SS-CNM (a); SnO₂ nanorods@SS-CNM (b); and NiO nanorods@SS-CNM (c); (d) Cycle life of MnO₂ nanorods@SS-CNM, SnO₂ nanorods@SS-CNM, and NiO nanorods@SS-CNM electrode materials at a scan rate of 0.1 V·s⁻¹ [79].

3. Conclusions

Some recent achievements on mesoporous transition metal oxides (RuO₂, MnO₂, NiO, Co₃O₄ and NiCo₂O₄) for applications in supercapacitors were selected and reviewed. From this research, one can see that much progress has been made in the past decade. High specific capacity and excellent stability of nanomaterials have been observed from some mesoporous materials. In order to make the electrochemical performance of each material chosen in this mini-review more clear, their highest specific capacitance values and synthetic methods from literature mentioned in this paper are listed in Table 2. In the following research, simple synthetic methods that can produce metal oxide nanomaterials with appropriate morphology and are suitable for large-scale production should be a continuous concern for the purpose of real supercapacitor devices. In addition, attention should also be focused on the design and synthesis of composite materials, such as transition metal oxides/metal, and transition metal oxides/active carbon, even on the combining of ionic liquids with mesoporous transition metal oxides. By doing so, the electrochemical performance of mesoporous transition metal oxide-based pseudo-capacitance could be improved substantially attributing to the synergistic effect of individual constituents. Especially, composite materials with 3D structures may provide more efficient and more rapid transportation for ions and electrons and thus result in higher electrochemical performance.

Table 2. The best special capacitances of each material.

Materials	Synthetic Method	Specific Capacitance (F·g ⁻¹)
RuO ₂	Sol-gel method	720 [18]
MnO ₂	Template method	297 [39]
NiO	Gydrothermal method	1700 [46]
Co ₃ O ₄	Sol-gel method followed by freeze-drying	742.3 [60]
Co ₃ O ₄ /Ni	Robust adhesion	2735–1471 [64]
NiCo ₂ O ₄	Sydrothermal method assisted by PVP and a post annealing treatment	1619.1 [72]
NiCo ₂ O ₄ /Ni	Hydrothermal method followed by annealing process	2623.3 [77]
RuO ₂ /Order mesoporous carbon	Soak followed by annealing	633 [4]
MnO ₂ /Mesopous silica supported carbon nanomembranes	<i>In situ</i> grown	964 [79]
NiO/Mesopous silica supported carbon nanomembranes	<i>In situ</i> grown	620 [79]
Co ₃ O ₄ /MWCNT	Chemical co-precipitation method	418 [80]

Acknowledgments

This work was supported by the National Natural Science Foundation of China (Grant No. 51273076 and No. 51473061), and the State Key Laboratory of Laser Interaction with Matter (Grant No. SKLLIM1403).

Author Contributions

Y. Wang and Y.-W. Yang wrote the first draft of the manuscript. Editing and revisions were carried out collaboratively by all the authors.

Conflicts of Interest

The authors declare no conflict of interest.

References

- Huang, L.; Chen, D.C.; Ding, Y.; Feng, S.; Wang, Z.L.; Liu, M.L. Nickel-cobalt hydroxide nanosheets coated on NiCo₂O₄ nanowires grown on carbon fiber paper for high-performance pseudocapacitors. *Nano Lett.* **2013**, *13*, 3135–3139.
- Wang, H.W.; Yi, H.; Chen, X.; Wang, X.F. One-step strategy to three-dimensional graphene/VO₂ nanobelt composite hydrogels for high performance supercapacitors. *J. Mater. Chem. A* **2014**, *2*, 1165–1173.
- Simon, P.; Gogotsi, Y. Materials for electrochemical capacitors, *Nat. Mater.* **2008**, *7*, 845–854.

4. Li, H.F.; Wang, R.D.; Cao, R. Physical and electrochemical characterization of hydrous ruthenium oxide/ordered mesoporous carbon composites as supercapacitor. *Microporous Mesoporous Mater.* **2008**, *111*, 32–38.
5. Wu, M.Q.; Gao, J.H.; Zhang, S.R.; Chen, A. Synthesis and characterization of aerogel-like mesoporous nickel oxide for electrochemical supercapacitors. *J. Porous Mater.* **2006**, *13*, 407–412.
6. Wang, G.P.; Zhang, L.; Zhang, J.J. A review of electrode materials for electrochemical supercapacitors. *Chem. Soc. Rev.* **2012**, *41*, 797–828.
7. Salunkhe, R.R.; Lin, J.J.; Malgras, V.; Dou, S.X.; Kim, J.H.; Yamauchi, Y. Large-scale synthesis of coaxial carbon nanotube/Ni(OH)₂ composites for asymmetric supercapacitor application. *Nano Energy* **2015**, *11*, 211–218.
8. Tan, J.; Salunkhe, R.R.; Liu, J.; Torad, N.L.; Imura, M.; Furukawa, S.; Yamauchi, Y. Thermal conversion of core-shell metal-organic frameworks: A new method for selectively functionalized nanoporous hybrid carbon. *J. Am. Chem. Soc.* **2015**, *137*, 1572–1580.
9. Salunkhe, R.R.; Tang, J.; Kamachi, Y.; Nakato, T.; Kim, J.H.; Yamauchi, Y. Asymmetric supercapacitors using 3D nanoporous carbon and cobalt oxide electrodes synthesized from a single metal-organic framework. *ACS Nano* **2015**, *9*, 6288–6296.
10. Tarascon, J.M.; Armand, M. Issues and challenges facing rechargeable lithium batteries. *Nature* **2001**, *414*, 359–367.
11. Whittingham, M.S. Lithium batteries and cathode materials. *Chem. Rev.* **2004**, *104*, 4271–4301.
12. Brezesinski, T.; Wang, J.; Tolbert, S.H.; Dunn, B. Ordered mesoporous α -MoO₃ with iso-oriented nanocrystalline walls for thin-film pseudocapacitors. *Nat. Mater.* **2010**, *9*, 146–151.
13. Conway, B.E. *Electrochemical Supercapacitors*; Kluwer Academic: New York, NY, USA, 1999.
14. Winter, M.; Brodd, R.J. What are batteries, fuel cells, and supercapacitors? *Chem. Rev.* **2004**, *104*, 4245–4269.
15. Aricò, A.S.; Bruce, P.; Scrosati, B.; Tarasco, J.; Schalkwijk, W. Nanostructured materials for advanced energy conversion and storage devices. *Nat. Mater.* **2005**, *4*, 366–377.
16. Conway, B.E. Transition from supercapacitor to battery behavior in electrochemical energy storage. *J. Electrochem. Soc.* **1991**, *138*, 1539–1548.
17. Augustyn, V.; Simon, P.; Dunn, B. Pseudocapacitive oxide materials for high-rate electrochemical energy storage. *Energy Environ. Sci.* **2014**, *7*, 1597–1614.
18. Zheng, J.P.; Cygan, P.J.; Jow, T.R. Hydrous ruthenium oxide as an electrode material for electrochemical supercapacitors. *J. Electrochem. Soc.* **1995**, *142*, 2699–2703.
19. Sun, S.M.; Wang, P.Y.; Wu, Q.; Wang, S.; Fang, S.M. Template-free synthesis of mesoporous MnO₂ under ultrasound irradiation for supercapacitor electrode. *Mater. Lett.* **2014**, *137*, 206–209.
20. Wang, Q.; Li, Z.S.; Huang, Y.G.; Li, Q.Y.; Wang, X.Y. A novel hybrid supercapacitor based on spherical activated carbon and spherical MnO₂ in a non-aqueous electrolyte. *J. Mater. Chem.* **2010**, *20*, 3883–3889.
21. Yuan, C.Z.; Li, J.Y.; Hou, L.R.; Lin, J.D.; Pang, G.; Zhang, L.H.; Lian, L.; Zhang, X.G. Template-engaged synthesis of uniform mesoporous hollow NiCo₂O₄ sub-microspheres towards high-performance electrochemical capacitors. *RSC Adv.* **2013**, *3*, 18573–18578.

22. Du, J.; Zhou, G.; Zhang, H.M.; Cheng, C.; Ma, J.M.; Wei, W.F.; Chen, L.B.; Wang, T.H. Ultrathin Porous NiCo₂O₄ Nanosheet Arrays on Flexible Carbon Fabric for High-Performance Supercapacitors. *ACS Appl. Mater. Interfaces* **2013**, *5*, 7405–7409.
23. Subramanian, V.; Hall, S.C.; Smith, P.H.; Rambabu, B. Mesoporous anhydrous RuO₂ as a supercapacitor electrode material. *Solid State Ionics* **2004**, *175*, 511–515.
24. Bi, R.R.; Wu, X.L.; Cao, F.F.; Jiang, L.Y.; Guo, Y.G.; Wan, L.J. Highly dispersed RuO₂ nanoparticles on carbon nanotubes: Facile synthesis and enhanced supercapacitance performance. *J. Phys. Chem. C* **2010**, *114*, 2448–2451.
25. Rakhi, R.B.; Chen, W.; Hedhili, M.N.; Cha, D.; Alshareef, H.N. Enhanced rate performance of mesoporous Co₃O₄ nanosheet supercapacitor electrodes by hydrous RuO₂ nanoparticle decoration. *ACS Appl. Mater. Interfaces* **2014**, *6*, 4196–4206.
26. Rochefort, D.; Dabo, P.; Guay, D.; Sherwood, P.M.A. XPS investigations of thermally prepared RuO₂ electrodes in reductive conditions. *Electrochim. Acta* **2003**, *48*, 4245–4252.
27. Galizzioli, D.; Tantardini, F.; Trasatti, S. Ruthenium dioxide: A new electrode material. 1. Behaviour in acid solutions of inert electrolytes. *J. Appl. Electrochem.* **1974**, *4*, 57–67.
28. Liu, T.C.; Pell, W.G.; Conway, B.E. Self-discharge and potential recovery phenomena at thermally and electrochemically prepared RuO₂ supercapacitor electrodes, *Electrochim. Acta* **1997**, *42*, 3541–3552.
29. Dubala, D.P.; Gund, G.S.; Holze, R.; Jadhav, H.S.; Lokhande, C.D.; Park, C.J. Solution-based binder-free synthetic approach of RuO₂ thin films for all solid state supercapacitors. *Electrochim. Acta* **2013**, *103*, 103–109.
30. Liu, X.M.; Zhang, X.G. NiO-based composite electrode with RuO₂ for electrochemical capacitors. *Electrochim. Acta* **2004**, *49*, 229–232.
31. Pusawale, S.N.; Deshmukh, P.R.; Gunjekar, J.L.; Lokhande, C.D. SnO₂-RuO₂ composite films by chemical deposition for supercapacitor application. *Mater. Chem. Phys.* **2013**, *139*, 416–422.
32. Li, X.; Gan, W.P.; Zheng, F.; Li, L.L.; Zhu, N.N.; Huang, X.Q. Preparation and electrochemical properties of RuO₂/polyaniline electrodes for supercapacitors. *Synth. Met.* **2012**, *162*, 953–957.
33. Wang, Y.G.; Zhang, X.G. Preparation and electrochemical capacitance of RuO₂/TiO₂ nanotubes composites. *Electrochim. Acta* **2004**, *49*, 1957–1962.
34. Liu, X.R.; Pickup, P.G. Ru oxide supercapacitors with high loadings and high power and energy densities. *J. Power Sources* **2008**, *176*, 410–416.
35. Song, Z.X.; Liu, W.; Zhao, M.; Zhang, Y.J.; Liu, G.C.; Yu, C.; Qiu, J.S. A facile template-free synthesis of α -MnO₂ nanorods for supercapacitor. *J. Alloys Compd.* **2013**, *560*, 151–155.
36. Yousefi, T.; Golikand, A.N.; Mashhadizadeh, M.H.; Aghazadeh, M. Template-free synthesis of MnO₂ nanowires with secondary flower like structure: Characterization and supercapacitor behavior studies. *Curr. Appl. Phys.* **2012**, *12*, 193–198.
37. Nayak, P.K.; Munichandraiah, N. Mesoporous MnO₂ synthesized by using a tri-block copolymer for electrochemical supercapacitor studies. *Microporous Mesoporous Mater.* **2011**, *143*, 206–214.
38. Zhou, Q.; Li, X.; Li, Y.G.; Tian, B.Z.; Zhao, D.Y.; Jiang, Z.Y. Synthesis and electrochemical properties of semicrystalline gyroidal mesoporous MnO₂. *Chin. J. Chem.* **2006**, *24*, 835–839.
39. Devaraj, S.; Gabriel, G.S.; Gajjela, S.R.; Balaya, P. Mesoporous MnO₂ and its capacitive behavior. *Electrochem. Solid-State Lett.* **2012**, *15*, A57–A59.

40. Nayak, P.K.; Munichandraiah, N. Rapid sonochemical synthesis of mesoporous MnO₂ for supercapacitor applications. *Mater. Sci. Eng. B* **2012**, *177*, 849–854.
41. Ming, B.S.; Li, J.L.; Kang, F.Y.; Pang, G.Y.; Zhang, Y.K.; Chen, L.; Xu, J.Y.; Wang, X.D. Microwave-hydrothermal synthesis of birnessite-type MnO₂ nanospheres as supercapacitor electrode materials. *J. Power Sources* **2012**, *198*, 428–431.
42. Kim, B.K.; Chabot, V.; Yu, A.P. Carbon nanomaterials supported Ni(OH)₂/NiO hybrid flower structure for supercapacitor. *Electrochim. Acta* **2013**, *109*, 370–380.
43. Yuan, C.Z.; Zhang, X.G.; Su, L.H.; Gao, B.; Shen, L.F. Facile synthesis and self-assembly of hierarchical porous NiO nano/micro spherical superstructures for high performance supercapacitors. *J. Mater. Chem.* **2009**, *19*, 5772–5777.
44. Lee, J.W.; Ahn, T.; Kim, J.H.; Ko, J.M.; Kim, J. Nanosheets based mesoporous NiO microspherical structures via facile and template-free method for high performance supercapacitors. *Electrochim. Acta* **2011**, *56*, 4849–4857.
45. Li, X.W.; Xiong, S.L.; Li, J.F.; Bai, J.; Qian, Y.T. Mesoporous NiO ultrathin nanowire networks topotactically transformed from Ni(OH)₂ hierarchical microspheres and their superior electrochemical capacitance properties and excellent capability for water treatment. *J. Mater. Chem.* **2012**, *22*, 14276–14283.
46. Yang, M.; Li, J.X.; Li, H.H.; Su, L.W.; Wei, J.P.; Zhou, Z. Mesoporous slit-structured NiO for high-performance pseudocapacitors. *Phys. Chem. Chem. Phys.* **2012**, *14*, 11048–11052.
47. Liu, F.; Yuan, W.; Li, T.Y.; Zhang, Z. Synthesis and electrochemical performance of mesoporous nickel oxide using mixed surfactant template. *Mater. Res. Innov.* **2015**, *19*, 70–75.
48. Wang, Y.L.; Chang, B.B.; Guan, D.X.; Pei, K.M.; Chen, Z.; Yang, M.; Dong, X.P. Preparation of nanospherical porous NiO by a hard template route and its supercapacitor application. *Mater. Lett.* **2014**, *135*, 172–175.
49. Meher, S.K.; Justin, P.; Rao, G.R. Microwave-mediated synthesis for improved morphology and pseudocapacitance performance of nickel oxide. *ACS Appl. Mater. Interfaces* **2011**, *3*, 2063–2073.
50. Kim, S.; Lee, J.; Ahn, H.; Song, H.; Jang, J. Facile route to an efficient NiO supercapacitor with a three-dimensional nanonetwork morphology. *ACS Appl. Mater. Interfaces* **2013**, *5*, 1596–1603.
51. Han, D.D.; Jing, X.Y.; Wang, J.; Yang, P.P.; Song, D.L.; Liu, J.Y. Porous lanthanum doped NiO microspheres for supercapacitor application. *J. Electroanal. Chem.* **2012**, *682*, 37–44.
52. Lu, Q.; Lattanzi, M.W.; Chen, Y.; Kou, X.; Li, W.; Fan, X.; Unruh, K.M.; Chen, J.G.; Xiao, J.Q. Supercapacitor electrodes with high-energy and power densities prepared from monolithic NiO/Ni nanocomposites. *Angew. Chem. Int. Ed.* **2011**, *50*, 6847–6850.
53. Yuan, C.Z.; Yang, L.; Hou, L.R.; Shen, L.F.; Zhang, F.; Li, D.K.; Zhang, X.G. Large-scale Co₃O₄ nanoparticles growing on nickel sheets via a one-step strategy and their ultra-highly reversible redox reaction toward supercapacitors. *J. Mater. Chem.* **2011**, *21*, 18183–18185.
54. Lee, K.K.; Chin, W.S.; Sow, C.H. Cobalt-based compounds and composites as electrode materials for high-performance electrochemical capacitors. *J. Mater. Chem. A* **2014**, *2*, 17212–17248.
55. Xiao, Y.H.; Zhang, A.Q.; Liu, S.J.; Zhao, J.H.; Fang, S.M.; Jia, D.Z.; Li, F. Free-standing and porous hierarchical nanoarchitectures constructed with cobalt cobaltite nanowalls for supercapacitors with high specific capacitances. *J. Power Sources* **2012**, *219*, 140–146.

56. Zhong, J.H.; Wang, A.L.; Li, G.R.; Wang, J.W.; Ou, Y.N.; Tong, Y.X. Co₃O₄/Ni(OH)₂ composite mesoporous nanosheet networks as a promising electrode for supercapacitor applications. *J. Mater. Chem.* **2012**, *22*, 5656–5665.
57. Cao, L.; Lu, M.; Li, H.L. Preparation of mesoporous nanocrystalline Co₃O₄ and its applicability of porosity to the formation of electrochemical capacitance. *J. Electrochem. Soc.* **2005**, *152*, A871–A875.
58. Wang, L.; Liu, X.H.; Wang, X.; Yang, X.J.; Lu, L.D. Preparation and electrochemical properties of mesoporous Co₃O₄ crater-like microspheres as supercapacitor electrode materials. *Curr. Appl. Phys.* **2010**, *10*, 1422–1426.
59. Yuan, Y.F.; Xia, X.H.; Wu, J.B.; Huang, X.H.; Pei, Y.B.; Yang, J.L.; Guo, S.Y. Hierarchically porous Co₃O₄ film with mesoporous walls prepared via liquid crystalline template for supercapacitor application. *Electrochem. Commun.* **2011**, *11*, 1123–1126.
60. Wang, X.; Sumboja, A.; Khoo, E.; Yan, C.Y.; Lee, P. Cryogel synthesis of hierarchical interconnected macro-/mesoporous Co₃O₄ with superb electrochemical energy storage. *J. Phys. Chem. C* **2012**, *116*, 4930–4935.
61. Liu, X.M.; Long, Q.; Jiang, C.H.; Zhan, B.B.; Li, C.; Liu, S.J.; Zhao, Q.; Huang, W.; Dong, X.C. Facile and green synthesis of mesoporous Co₃O₄ nanocubes and their applications for supercapacitors. *Nanoscale* **2013**, *5*, 6525–6529.
62. Yan, D.L.; Zhang, H.; Chen, L.; Zhu, G.S.; Li, S.C.; Xu, H.R.; Yu, A.B. Biomorphic synthesis of mesoporous Co₃O₄ microtubules and their pseudocapacitive performance. *ACS Appl. Mater. Interfaces* **2014**, *6*, 15632–15637.
63. Xiong, S.L.; Yuan, C.Z.; Zhang, X.G.; Xi, B.J.; Qian, Y.T. Controllable synthesis of mesoporous Co₃O₄ nanostructures with tunable morphology for application in supercapacitors. *Chem. Eur. J.* **2009**, *15*, 5320–5326.
64. Yuan, C.Z.; Yang, L.; Hou, L.R.; Shen, L.F.; Zhang, X.G.; Lou, X.W. Growth of ultrathin mesoporous Co₃O₄ nanosheet arrays on Ni foam for high-performance electrochemical capacitors. *Energy Environ. Sci.* **2012**, *5*, 7883–7887.
65. Zhi, J.; Deng, S.; Zhang, Y.X.; Wang, Y.F.; Hu, A.G. Embedding Co₃O₄ nanoparticles in SBA-15 supported carbon nanomembrane for advanced supercapacitor materials. *J. Mater. Chem. A* **2013**, *1*, 3171–3176.
66. Padmanathan, N.; Selladurai, S.; Razeeb, K.M. Ultra-fast rate capability of a symmetric supercapacitor with a hierarchical Co₃O₄ nanowire/nanoflower hybrid structure in nonaqueous electrolyte. *RSC Adv.* **2015**, *5*, 12700–12709.
67. Xu, K.B.; Zou, R.J.; Li, W.Y.; Xue, Y.F.; Song, G.S.; Liu, Q.; Liu, X.J.; Hu, J.Q. Self-assembling hybrid NiO/Co₃O₄ ultrathin and mesoporous nanosheets into flower-like architectures for pseudocapacitance. *J. Mater. Chem. A* **2013**, *1*, 9107–9113.
68. Wei, T.Y.; Chen, C.H.; Chien, H.C.; Lu, S.Y.; Hu, C.C. A cost-effective supercapacitor material of ultrahigh specific capacitances: Spinel nickel cobaltite aerogels from an epoxide-driven sol-gel process. *Adv. Mater.* **2010**, *22*, 347–351.
69. Wu, Z.B.; Zhu, Y.R.; Ji, X.B. NiCo₂O₄-based materials for electrochemical supercapacitors. *J. Mater. Chem. A* **2014**, *2*, 14759–14772.

70. Yuan, C.Z.; Li, J.Y.; Hou, L.R.; Yang, L.; Shen, L.F.; Zhang, X.G. Facile template-free synthesis of ultralayered mesoporous nickel cobaltite nanowires towards high-performance electrochemical capacitors. *J. Mater. Chem.* **2012**, *22*, 16084–16090.
71. Padmanathan, N.; Selladurai, S. Solvothermal synthesis of mesoporous NiCo₂O₄ spinel oxide nanostructure for high-performance electrochemical capacitor electrode. *Ionics* **2013**, *19*, 1535–1544.
72. Zhang, Y.F.; Ma, M.Z.; Yang, J.; Su, H.Q.; Huang, W.; Dong, X.C. Selective synthesis of hierarchical mesoporous spinel NiCo₂O₄ for high-performance supercapacitors. *Nanoscale* **2014**, *6*, 4303–4308.
73. Hsu, C.T.; Hu, C.C. Synthesis and characterization of mesoporous spinel NiCo₂O₄ using surfactant-assembled dispersion for asymmetric supercapacitors. *J. Power Sources* **2013**, *242*, 662–671.
74. Zhu, Y.R.; Wu, Z.B.; Jing, M.J.; Song, W.X.; Hou, H.S.; Yang, X.M.; Chen, Q.Y.; Ji, X.B. 3D network-like mesoporous NiCo₂O₄ nanostructures as advanced electrode material for supercapacitors. *Electrochim. Acta* **2014**, *149*, 144–151.
75. Yu, M.; Chen, J.P.; Liu, J.H.; Li, S.M.; Ma, Y.X.; Zhang, J.D.; An, J.W. Mesoporous NiCo₂O₄ nanoneedles grown on 3D graphene-nickel foam for supercapacitor and methanol electro-oxidation. *Electrochim. Acta* **2015**, *151*, 99–108.
76. Zheng, Q.Y.; Zhang, X.Y.; Shen, Y.M. Construction of hierarchical porous NiCo₂O₄ films composed of nanowalls as cathode materials for high-performance supercapacitor. *Mater. Res. Bull.* **2015**, *64*, 401–404.
77. Zhou, Q.W.; Xing, J.C.; Gao, Y.F.; Lv, X.J.; He, Y.M.; Guo, Z.H.; Li, Y.M. Ordered assembly of NiCo₂O₄ multiple hierarchical structures for high-performance pseudocapacitors. *ACS Appl. Mater. Interfaces* **2014**, *6*, 11394–11402.
78. Fu, H.Y.; Wang, Z.Y.; Li, Y.H.; Zhang, Y.F. Electrochemical deposition of mesoporous NiCo₂O₄ nanosheets on Ni foam as highperformance electrodes for supercapacitors. *Mater. Res. Innov.* **2015**, *19*, S255–S259.
79. Zhi, J.; Deng, S.; Wang, Y.F.; Hu, A.G. Highly ordered metal oxide nanorods inside mesoporous silica supported carbon nanomembranes: High performance electrode materials for symmetrical supercapacitor devices. *J. Phys. Chem. C* **2015**, *119*, 8530–8536.
80. Lang, J.W.; Yan, X.B.; Xue, Q.J. Facile preparation and electrochemical characterization of cobalt oxide/multi-walled carbon nanotube composites for supercapacitors. *J. Power Sources* **2011**, *196*, 7841–7846.
81. Dong, X.P.; Shen, W.H.; Gu, J.L.; Xiong, L.M.; Zhu, Y.F.; Li, H.; Shi, J.L. MnO₂-embedded-in-mesoporous-carbon-wall structure for use as electrochemical capacitors. *J. Phys. Chem. B* **2006**, *110*, 6015–6019.
82. Li, G.R.; Feng, Z.P.; Ou, Y.N.; Wu, D.C.; Fu, R.W.; Tong, Y.X. Mesoporous MnO₂/carbon aerogel composites as promising electrode materials for high-performance supercapacitors. *Langmuir* **2010**, *26*, 2209–2213.
83. Liu, M.X.; Gan, L.H.; Xiong, W.; Xu, Z.J.; Zhu, D.Z.; Chen, L.W. Development of MnO₂/porous carbon microspheres with a partially graphitic structure for high performance supercapacitor electrodes. *J. Mater. Chem. A* **2014**, *2*, 2555–2562.

84. Kiani, M.A.; Khani, H.; Mohammadi, N. MnO₂/ordered mesoporous carbon nanocomposite for electrochemical supercapacitor. *J. Solid State Electrochem.* **2014**, *18*, 1117–1125.
85. Cao, P.Q.; Wang, L.C.; Xu, Y.J.; Fu, Y.B.; Ma, X.H. Facile hydrothermal synthesis of mesoporous nickel oxide/reduced graphene oxide composites for high performance electrochemical supercapacitor. *Electrochim. Acta* **2015**, *157*, 359–368.

© 2015 by the authors; licensee MDPI, Basel, Switzerland. This article is an open access article distributed under the terms and conditions of the Creative Commons Attribution license (<http://creativecommons.org/licenses/by/4.0/>).